Theor Chem Acc (2011) 129:303–312
DOI 10.1007/s00214-010-0775-x

REGULAR ARTICLE

DFT studies of reductive elimination, C–H activation and β-hydride elimination in alkyl and aryl palladium amine complexes

Christopher Ryan · Alexandra K. de K. Lewis · Stephen Caddick · Nikolas Kaltsoyannis

Received: 14 April 2010 / Accepted: 6 June 2010 / Published online: 26 June 2010

Abstract The factors affecting C–N bond formation via reductive elimination from Pd(I^{t}Bu)(neopentyl)(morpholide) (I^{t}Bu = 1,3-Di-tert-butyl-imidazol-2-ylidene) are studied computationally. DFT calculations indicate that choosing an alkyl group without β hydrides, such as neopentyl, has a detrimental effect on the possibility of C–N reductive elimination. In the absence of β hydride elimination, a pathway of lower energy than reductive elimination is found, namely morpholide-promoted C–H activation of neopentyl ^{t}Bu has a significantly lower activation energy than reductive elimination. Changing the ancillary ligand from I^{t}Bu to tricyclopentylphosphine (P(Cyp)$_3$) has little impact. By contrast, replacing neopentyl by phenyl leads to a c. 50% reduction in activation energy. Study of Pd(I^{t}Bu)(2-methylpropyl)(morpholide) permits comparison of the potential energy surfaces for three possible processes; (1) reductive elimination (2) morpholide-promoted C–H activation and (3) β-hydride elimination and reveals that the activation energies for these processes increase in the order of (3) < (2) < (1).

Keywords Palladium · Organometallic · Reductive elimination · Beta hydride elimination · C–H activation · NHC

Dedicated to Professor Pekka Pyykkö on the occasion of his 70th birthday and published as part of the Pyykkö Festschrift Issue.

Electronic supplementary material The online version of this article (doi:10.1007/s00214-010-0775-x) contains supplementary material, which is available to authorized users.

C. Ryan · A. K. de K. Lewis · S. Caddick · N. Kaltsoyannis (✉)
Department of Chemistry, University College London, 20 Gordon Street, London WC1H 0AJ, UK
e-mail: n.kaltsoyannis@ucl.ac.uk

1 Introduction

C–C and C–N bond–forming reactions are the key steps in the synthesis of many organic substances [1, 2]. The use of Pd as a catalyst in these types of reactions is very well documented and has become an extremely important tool in modern day synthesis. Yet, whilst Suzuki [3–5], Negishi [6–9], Heck [10], Kumada [11–13], and Buchwald–Hartwig amination [14, 15] reactions have been successfully employed using aryl halides, the corresponding alkyl halides in the same transformations have remained, until recently, much more challenging. Historically, the presence of β-hydrogens on the alkyl substituent–created problems with β-hydride elimination (Scheme 1), although this problem was overcome by Suzuki [16], Fu and Zhou [17], Kambe [18], Beller [19] and Knochel [20]. However, even with these recent advances in (sp^3)C–C coupling, extension to (sp^3)C–heteroatom bond formation has proved demanding.

We have previously reported efforts towards developing a new protocol for catalytic alkyl amination reactions employing *N*-heterocyclic carbene (NHC)–Pd complexes as catalysts. In order to maximise C–N bond formation, we employed the NHC I^{t}Bu, together with neopentyl chloride. McGuinness and Cavell et al. [21]. have shown that sterically demanding substituents on metal-bound NHC ligands hinder the close approach of alkyl groups to the NHC, so the ^{t}Bu groups on the NHC should inhibit unwanted reaction with the neopentyl unit. We also reasoned that the steric bulk of the neopentyl would prevent direct S_N2 attack by the amine, and hence that the favoured reaction would be the (sp^3)C–N reductive elimination from the metal-bound alkyl and amide.

Despite these precautions, our efforts resulted in the isolation of a square planar alkyl trans amination product

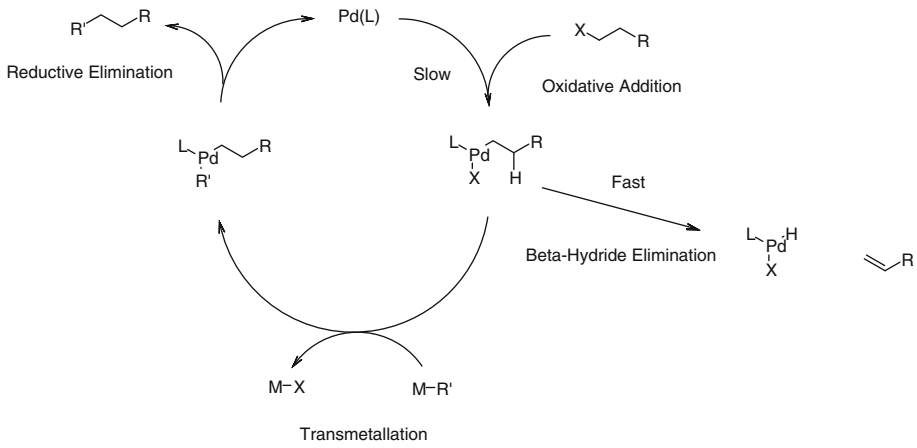

Scheme 1 Proposed mechanism for alkyl-amine cross-coupling reactions, comparing potential β-hydride elimination with reductive elimination

[Pd(neopentyl)(I^tBu)(morpholine)Cl] **1** [22, 23]. This complex proved remarkably stable and did not undergo reductive elimination despite having the required *cis* geometry. Furthermore, no evidence was found to suggest that deprotonation of the coordinated amine occurred when a variety of bases were added (KO^tBu, LHMDS, NaH, $NaOCEt_3$).

It is important to understand why the reductive elimination does not take place and, in the present contribution, we report computational efforts towards this goal. While previous computational studies have been carried out for complete Pd cross-coupling reactions [9, 24–32], as well as the individual oxidative addition [33–44], transmetallation [45–50] and reductive elimination steps [51–54], (sp^3)C–N alkyl amination has been less well studied. Previous theoretical work in this area includes a density functional theory (DFT) study of the oxidative addition of methyl chloride to a mono-ligated Pd(NHC) complex (NHC = *N*-1,3-di-tert-butyl-imidazol-2-ylidene) [25], and an investigation of the reductive elimination of methylamine from three and four coordinate complexes $Pd(PH_3)_{1\ or\ 2}(Me)(NH_2)$ [54].

In the present work, we explore several factors relating to reductive elimination of alkyl palladium amine complexes and we consider comparisons between aryl and alkyl amination, with emphasis on the reductive elimination step. Unlike previous work, we make no simplifications of the target molecules; NHC and phosphine ligands are modelled fully, as are the alkyl groups (dimethylpropyl and neopentyl) and amine (morpholine). I^tBu complexes are compared with those containing trialkyl phosphine ($PCyp_3$) groups, to establish if changes in the ancillary ligand can influence significantly the reaction energetics. As illustrated by Fu et al. [17], reductive elimination of alkyl palladium complexes can be effected even in the presence of β hydrogens, and the competition between β hydride elimination and reductive elimination in complexes containing an alkyl group containing β hydrogens is studied here. Also presented are data supporting the formation of a Pd–metallacycle via C–H activation of neopentyl ^{t}Bu and its subsequent effects on the reaction pathway.

2 Computational details

Density functional theory calculations were performed using the Amsterdam density functional [55] (ADF) quantum chemistry package with the PBE [56, 57] generalised gradient approximation (GGA) exchange correlation functional, which we have previously found to perform well in calculations on a wide range of compounds containing heavy metal atoms [58–62]. TZ2P zero-order regular approximation (ZORA) all electron basis sets were used on all atoms. Scalar relativistic effects were accounted for by the ZORA. The integration grid parameter was set to 6.0, and the geometry convergence was 10^{-3} au $Å^{-1}$. All geometries were optimised without symmetry constraints. Analytical harmonic frequency calculations were used to characterise stationary points as either true minima or transition states by the observation of 0 or 1 imaginary vibrational modes, respectively. Solvent effects (tetrahydrofuran) were included by the COnductor-like Screening MOdel [63, 64] (COSMO) with the following values for the atomic radii: Pd = 2.3 Å, O = 1.72 Å, Cl = 2.05 Å, N = 1.83 Å, P = 2.0 Å, C = 2.0 Å and H = 1.3 Å. The solvent radius and dielectric constant used were $r = 3.18$ Å and $\varepsilon = 7.58$. Zero point energy, and entropic and internal energy (298.15 K), corrections were taken from gas phase calculations and applied to both gas phase and solvent optimised minima and transition states. When calculating the zero point energies and thermodynamic corrections for the transition states, the single imaginary vibration was ignored. It should be noted that as some of the calculated reaction steps involve association or dissociation (i.e. a change in the number of species), the gas phase entropies lead to an overestimate of the reaction free

energies for associative steps (i.e. are too positive), and an underestimate for dissociative steps (i.e. are too negative), on account of restricted translational and rotational energies in solution. The relative free energies of activation are not affected by this.

3 Results and discussion

We began by optimising the geometry of **1** and were pleased that all four bond lengths involving the Pd atom deviated by at most 0.05 Å from their experimental value [23]. Loss of HCl from square planar **1** leads to **2**, which has a distorted T-shaped geometry due to the steric bulk of the neopentyl group. Here I^{t}Bu is *trans* to the morpholide, possibly as a result of the greater *trans* influence of the strongly electron donating neopentyl group. It is believed that **2** is the species from which reductive elimination takes place [25], and Fig. 1 presents a relative energy level diagram for the stationary points on the potential energy surface for this process. In order to facilitate elimination, the neopentyl group must rotate through c. 90° around the Pd–C bond to form complex **3**, at a cost of +8.1 kJ mol^{-1}. Further movement of the neopentyl group towards the morpholide leads to a reduction in the neopentyl-Pd-morpholide bond angle and hence to transition state **TS-4**, +122.9 kJ mol^{-1} higher in energy than **3**. The neopentyl group then passes to the N of the morpholide (**5**), and the reduction in the strain associated with the tri-cyclic core of the transition state, together with the location of the sterically cumbersome neopentyl group away from the I^{t}Bu tertiary butyl groups, results in a very significant reduction in energy (−147.2 kJ mol^{-1}). Combined with the dissociation of neopentyl morpholine **7,** this process is −166.6 kJ mol^{-1} exothermic with respect to the transition state **TS-4,** and 35.6 kJ mol^{-1} more stable than the three-coordinate Pd species **2**.

Addition of I^{t}Bu to Pd(I^{t}Bu) **6** leads to the formation of Pd(I^{t}Bu)$_2$ **8**, with an associated change in energy of −102.9 kJ mol^{-1}. The reverse of this process, the dissociation of I^{t}Bu from Pd(I^{t}Bu)$_2$ **8**, is known to occur at the beginning of many Pd(0)-catalysed cycles [65], and hence there is no obvious reason why, on the basis of Fig. 1, the reductive elimination stage of the alkyl amination reaction (via **TS-4**) should not take place. We therefore decided to probe the relative energetics of the reductive elimination when (1) the neopentyl group is replaced with phenyl (for which the reductive elimination is known to take place) and

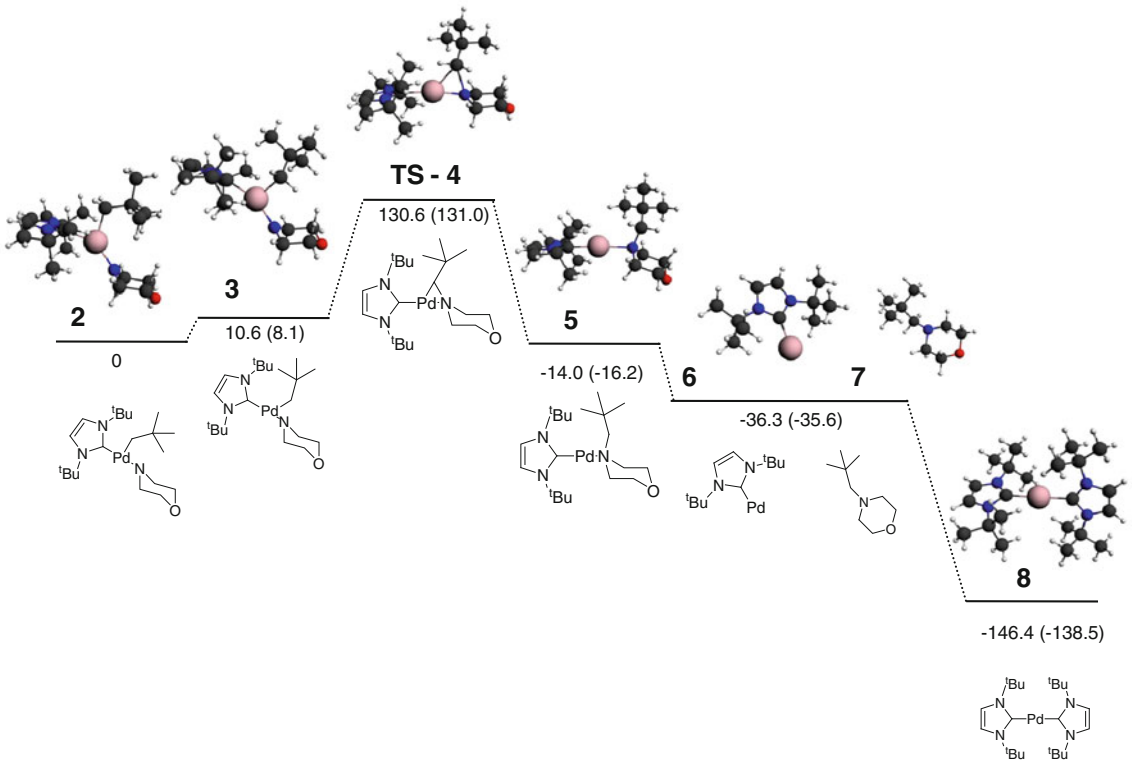

Fig. 1 Calculated relative energy level diagram (kJ mol^{-1}) of the stationary points on the potential energy surface for reductive elimination from **2**. The energies quoted are gas phase, including zero point, thermal and entropic corrections (at 298.15 K). Values in parentheses are derived from electronic energies computed with the inclusion of solvent effects, with zero point energies, thermal and entropic corrections taken from the gas phase calculations

(2) the strongly σ donating I^{t}Bu is replaced with a less donating trialkyl phosphine ($PCyp_3$). The results of these calculations are summarised in Fig. 2. Replacement of I^{t}Bu in **2** by $PCyp_3$ yields an activation energy from **13** to **TS-14** still well in excess of +100 kJ mol^{-1}. By contrast, the activation energy from **9**, the three-coordinate phenyl complex, is only +60.1 kJ mol^{-1} (to **TS-10**) in solution, substantially lower than the analogous steps on either the I^{t}Bu or phosphine neopentyl surfaces.

Table 1 collects some key bond length data for the structures discussed earlier. In the I^{t}Bu/neopentyl system, the Pd–N distance shortens significantly from the four coordinate species **1** to the three-coordinate **2**, before lengthening slightly in **TS-4** and then more significantly in **5**. There is little difference in the Pd–C(neopentyl) distance between the four- and three-coordinate species, but a very significant lengthening in **TS-4**. By contrast, there is little change in the Pd–C (I^{t}Bu) distance from **1** to **5**.

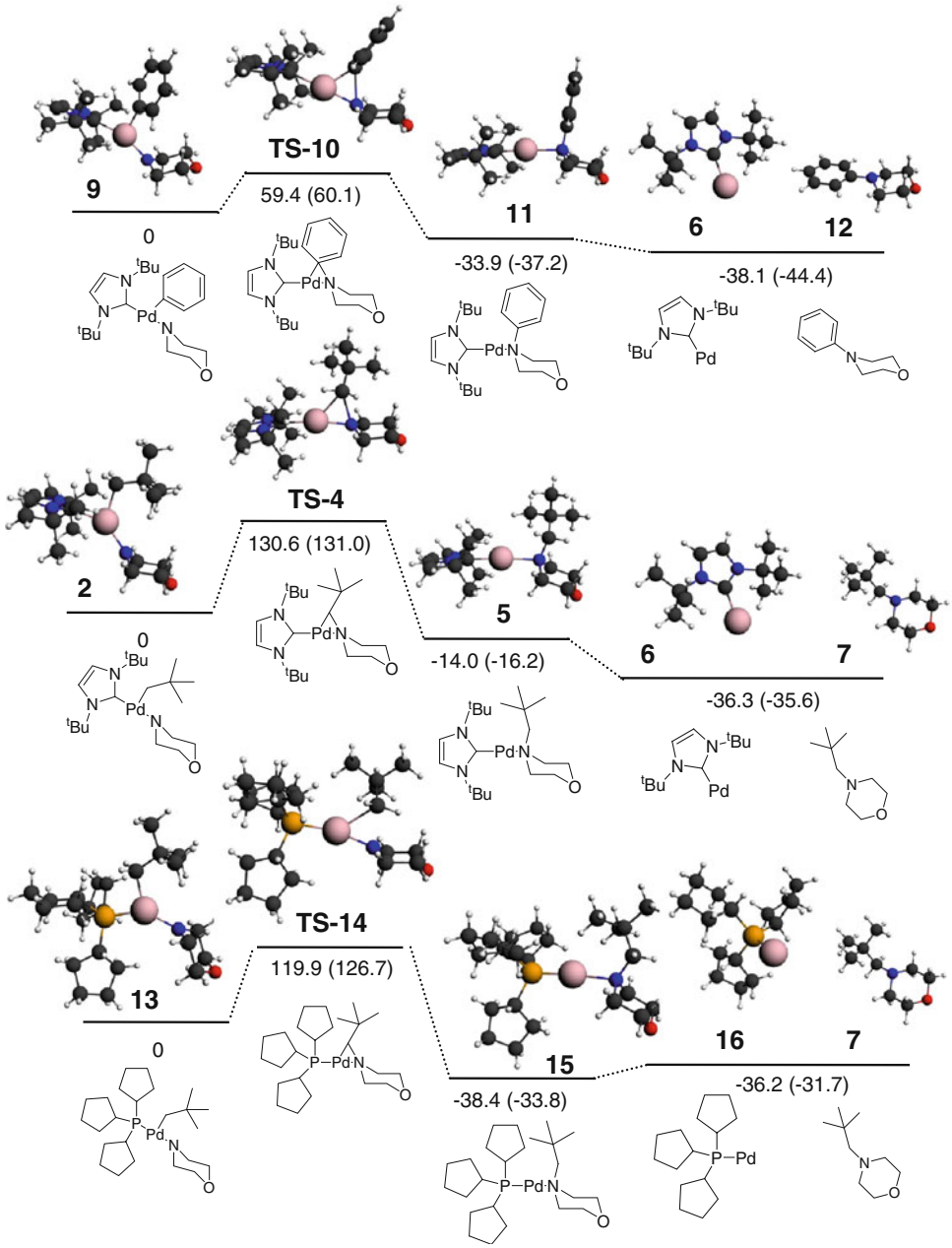

Fig. 2 Calculated relative energy level diagram (kJ mol^{-1}) of the stationary points on the potential energy surface for reductive elimination from (I^{t}Bu)Pd(phenyl)(morpholide) **9**, (I^{t}Bu)Pd(neopentyl)(morpholide) **2** and ($PCyp_3$)Pd(neopentyl)(morpholide) **13**. The energies quoted are gas phase, including zero point, thermal and entropic corrections (at 298.15 K). Values in parentheses are derived from electronic energies computed with the inclusion of solvent effects, with zero point energies, thermal and entropic corrections taken from the gas phase calculations

Table 1 Pd–ligand bond lengths (Å) and Mayer bond orders (in parentheses) for selected stationary points on the potential energy surfaces shown in Figs. 2 and 4

Pd(I^{t}Bu)(neopentyl)(morpholide) complexes				
Bond	**1**	**2**	**TS-4**	**5**
Pd–N	2.170	2.004 (0.83)	2.026 (0.59)	2.250 (0.32)
Pd–C(neopentyl)	2.120	2.097 (0.78)	2.408 (0.45)	–
C–N		(0.12)	(0.47)	(0.86)
Pd–C(I^{t}Bu)	2.000	2.037	2.036	1.985
Pd(I^{t}Bu)(phenyl)(morpholide) complexes				
Bond		**9**	**TS-10**	**11**
Pd–N		1.993 (0.87)	2.017 (0.55)	2.210 (0.31)
Pd–C(phenyl)		2.011 (0.85)	2.071 (0.66)	–
C–N		(0.11)	(0.49)	(0.95)
Pd–C(I^{t}Bu)		2.031	2.049	1.988
Pd(PCyp$_3$)(neopentyl)(morpholide) complexes				
Bond		**13**	**TS-14**	**15**
Pd–N		2.007 (0.83)	2.037 (0.57)	2.294 (0.27)
Pd–C(neopentyl)		2.075 (0.80)	2.436 (0.39)	–
C–N		(0.10)	(0.49)	(0.86)
Pd–P		2.239	2.522	2.199
Pd(I^{t}Bu)(2-methylpropyl)(morpholide) complexes				
Bond		**22**	**TS-23**	**24**
Pd–N		1.988 (0.87)	2.019 (0.56)	2.242 (0.32)
Pd–C(2-methylpropyl)		2.091 (0.81)	2.346 (0.39)	–
C–N		(0.10)	(0.51)	(0.85)
Pd–C(I^{t}Bu)		2.012	2.033	1.986

The analogous bond lengths in the PCyp$_3$ system behave similarly, with an increase in the Pd–N distance from **13** to **15** and a reduction in Pd–P. There is also a significant lengthening in the Pd–C distance on going from the three-coordinate **13** to the transition **TS-14**, such that the Pd–C(neopentyl) distances in **TS-4** and **TS-14** are rather similar, c. 2.4 Å. The distances in the phenyl complexes are similar to their equivalents in the neopentyl compounds, with the notable exception of the Pd–C(phenyl). Whereas the analogous bond in the neopentyl complexes is lengthened very significantly in **TS-4** and **TS-14** relative to the preceding three-coordinate minima, that in **TS-10** is only 0.06 Å longer than in **9**.

It is of interest to examine the possible causes of the differences between the neopentyl and phenyl systems. The much higher activation energy in the neopentyl systems may well result from steric factors. **2** is somewhat distorted from T-shaped on account of the steric bulk of the neopentyl group and hence, as discussed earlier, the neopentyl group must rotate in order to bring the neopentyl and morpholide ligands into sufficiently close proximity. This rotation is accompanied by the unwanted clash of the ^{t}Bu groups of the NHC with those of the neopentyl, and the combination of this congestion and the initial rotation may well have a significant effect on the energy of **TS-4**. Furthermore, the energy released on forming the two-coordinate species **5**, **15** and **11** from the preceding transition states is c. 50% greater for the neopentyl systems, indicative of larger steric congestion in the neopentyl transition states **TS-4** and **TS-14** relative to the phenyl **TS-10**.

In order to probe further the role of steric effects, we have recalculated the NHC/neopentyl surface, replacing the neopentyl group with a methyl ligand. The activation energy is reduced to +102.9 kJ mol^{-1} in solution; clearly sterics cannot account for all of the neopentyl/phenyl difference.

Table 1 reports Mayer bond orders (MBOs) [66, 67], in addition to the bond length data discussed earlier. MBOs contain all of the contributions to a bond between two atoms, i.e. they take account of all bonding and antibonding interactions in a single number. MBOs have been applied to a variety of systems by, for example, Bridgeman et al. [68]. The MBOs in Table 1 are, in general, rather similar in analogous complexes, with the exception of the Pd–C bond which weakens over the transition states. Specifically, the MBO for the weakening Pd–C bond in **TS-10** is significantly larger than for **TS-4** and **TS-14**, suggesting that the Pd–phenyl bond in **TS-10** is stronger than the Pd–alkyl bonds in the analogous transition states (the MBO for the Pd–C(Me) bond in the I^{t}Bu/methyl transition state is the same as the Pd–C(neopentyl) MBO in **TS-4**). The stronger Pd–C(phenyl) bonding in the transition state, consistent with the shorter Pd–C bond in **TS-10** *vs* **TS-4** and **TS-14**, contributes significantly to the reduced activation energy on the phenyl surface. It should also be noted that, in agreement with the idea that reduced electron density at the metal centre should promote reductive elimination, the Hirshfeld charge for the Pd atom is +0.37 in **2** and +0.83 in **9**.

With respect to the reductive elimination of an aryl substituent, no other low energy pathway is available. However, **3** has three ^{t}Bu groups, two from the NHC and one from the neopentyl ligand. Several studies involving neopentyl-bound group ten metals have shown C–H activation to be a viable process, often resulting in loss of 1,1-bis-dimethylcyclopropane from a metallocyclobutyl intermediate [69–71], a process which neighbouring group participation by the nitrogen of morpholide would facilitate. Therefore, further computational studies were carried

out to identify a mechanistic hypothesis to support the transfer of a hydrogen from neopentyl to the morpholide of Pd(I^tBu)(neopentyl)(morpholide) resulting in subsequent dissociation of morpholine, followed by the loss of the neopentyl group and formation of Pd(I^tBu)$_2$. The results are shown in Fig. 3.

The pathway begins with the transfer of a hydrogen atom from one of the neopentyl ^{t}Bu groups to the Pd centre, resulting in **TS-17**, a five coordinate Pd species consisting of bound I^tBu, morpholide, hydride, and the Pd centre incorporated in a metallocyclobutyl ring. The hydrogen lies in the same plane as the morpholide N and the neopentyl C atom to which it was previously bonded. Attempts to locate analogous transition states which do not involve the morpholide N proved unsuccessful, strongly suggesting that for the current system the presence of the N as a hydrogen acceptor is required. **TS-17** lies c. +88 kJ mol^{-1} higher in energy than **2**, some 43 kJ mol^{-1} lower than the barrier for reductive elimination (**TS-4**, Fig. 1). Furthermore **2** is well set up for the C–H activation process to take place, whereas for reductive elimination, rotation of the bulky neopentyl group is first required. Additionally, the free rotation of the ^{t}Bu group means that there are nine possible sites for C–H activation, compared with the one C centre for reductive elimination.

From **TS-17**, movement of the hydrogen towards the N of the morpholide results in **18**, a four coordinate Pd species of similar energy to the starting complex **2**. Rotation and dissociation of morpholine, followed by loss of 1,1-bis-dimethylcyclopropane, gives Pd(I^tBu) **6**, −50.5 kJ mol^{-1} more stable than **2**. Addition of I^tBu then gives **8**, as in Fig. 1.

Figures 1 and 3 suggest that reductive elimination is unfavourable in comparison with C–H activation, a situation which will be further exacerbated by the 9:1 ratio of C–H activation:reductive elimination sites. However, the neopentyl compound does not possess β-hydrogens, and we therefore decided to investigate the possible reaction pathways for a compound analogous to **2** which contains such hydrogens, Pd(I^tBu)(2-methylpropyl)(morpholide). This allows us to compare the potential surfaces not only for C–H activation and reductive elimination but also for β-hydride elimination.

Figure 4 shows the potential energy surface for reductive elimination of 2-methylpropyl morpholine from Pd(I^tBu)(2-methylpropyl)(morpholide) **22**. Comparison of Figs. 1 and 4 shows that the reductive elimination pathways for **2** and **22** are rather similar. From the distorted T-shaped **22**, 24 kJ mol^{-1} less is required to reach the transition state for reductive elimination, **TS-23**, than on the equivalent surface

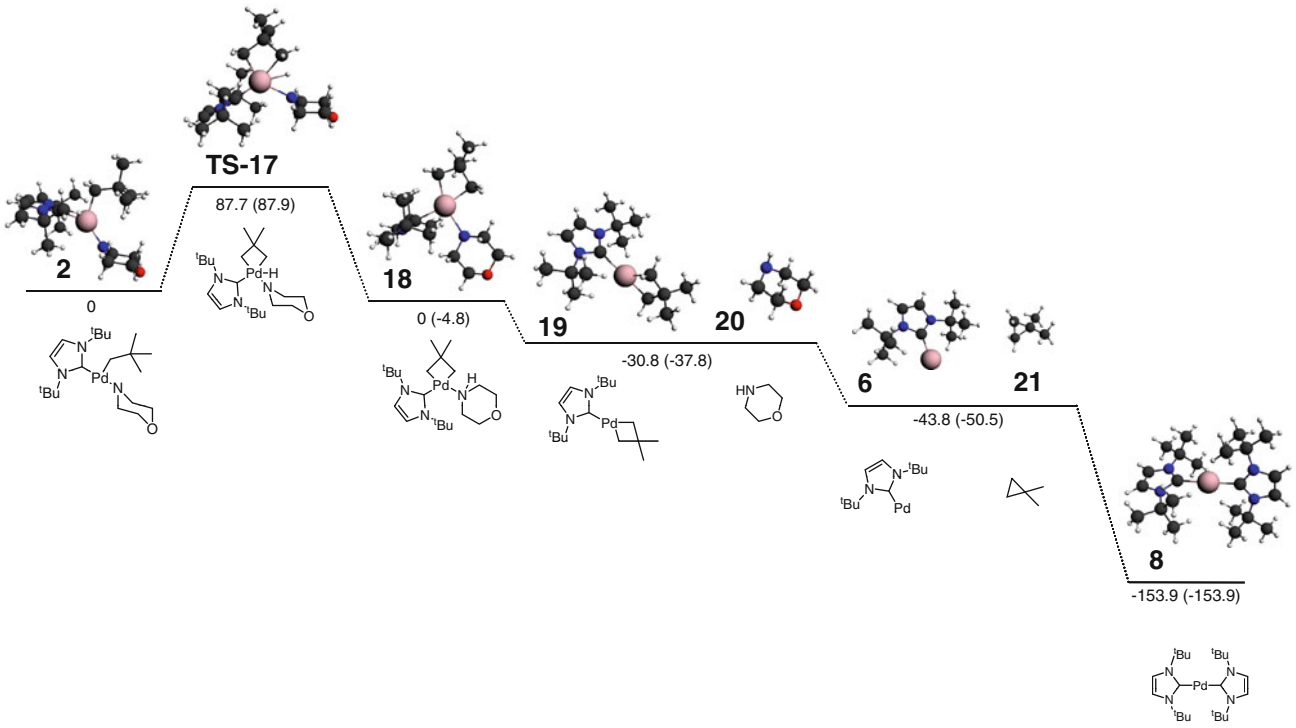

Fig. 3 Calculated relative energy level diagram (kJ mol^{-1}) of the stationary points on the potential energy surface for morpholide-promoted C–H activation of ^{t}Bu in **2**. The energies quoted are gas phase, including zero point, thermal and entropic corrections (at 298.15 K). Values in parentheses are derived from electronic energies computed with the inclusion of solvent effects, with zero point energies, thermal and entropic corrections taken from the gas phase calculations

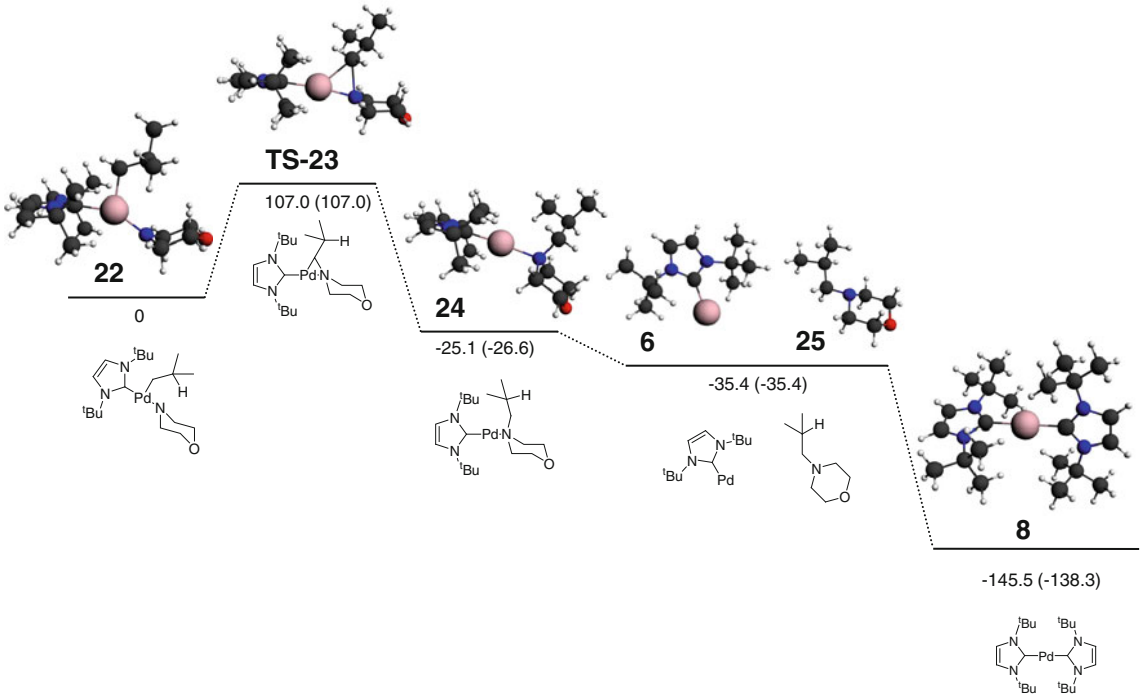

Fig. 4 Calculated relative energy level diagram (kJ mol^{-1}) of the stationary points on the potential energy surface for the reductive elimination of 2-methylpropyl morpholine from Pd(I^tBu)(2-methylpropyl)(morpholide) **22**. The energies quoted are gas phase, including zero point, thermal and entropic corrections (at 298.15 K). Values in parentheses are derived from electronic energies computed with the inclusion of solvent effects, with zero point energies, thermal and entropic corrections taken from the gas phase calculations

for neopentyl, possibly because there is one methyl group fewer in the 2-methylpropyl system and hence reduced steric congestion in the transition state. From **TS-23** the transfer of 2-methylpropyl to the morpholide N can take place, reducing Pd(II) to Pd(0) and lengthening the now Pd–morpholine bond from 2.019 to 2.242 Å (Table 1). This is strongly exothermic (−133.6 kJ mol^{-1} in THF solution) and subsequent loss of 2-methylpropyl morpholine and addition of I^tBu yields Pd(I^tBu)$_2$ **8**.

The second process considered earlier for **2** is the morpholide-promoted C–H activation of ^{t}Bu. To establish the effects of removing one of the three methyl groups from neopentyl on this process, we have calculated a potential surface analogous to that shown in Fig. 3 but for the 2-methylpropyl system **22**, and the results are presented in Fig. 5. As with the reductive elimination, comparison of Figs. 3 and 5 reveals rather similar surfaces. Indeed, the activation energy from **22** to **TS-26** is almost exactly the same as that between **2** and **TS-17** for the neopentyl system. That said, it might be expected that there is a rather larger dependence on the orientation of the alkyl group in **22** than in **2**, in that C–H activation requires a 2-methylpropyl methyl group to be adjacent to the morpholide N atom. There are, of course, only six such C–H bonds versus the nine in **2**.

A third possible reaction of **22** is β-hydride elimination from 2-methylpropyl, and the potential surface for this process is shown in Fig. 6. The activation energy to form **TS-30** is only +70.8 kJ mol^{-1} in solution, compared with +107.0 kJ mol^{-1} for reductive elimination (**TS-23**—Fig. 4) and +92.6 kJ mol^{-1} for morpholide-promoted C–H activation (**TS-26**—Fig. 5). Following β-hydride transfer, loss of either alkene or morpholine from complex **31** is possible. We find that the most favourable reaction is loss of morpholine to form **32** (−71.7 kJ mol^{-1}), a result of the stronger bonding between Pd and the alkene (confirmed by calculation of the metal–alkene interaction energy (−199.9 kJ mol^{-1}) compared with the metal–morpholine interaction energy (−32.3 kJ mol^{-1})). This is consistent with our observation that a β-hydride transition state could be located only for morpholide-assisted loss of hydride.

It would therefore appear that the most energetically favourable reaction of **22** is β-hydride elimination. The bulky 2-methylpropyl group impedes the formation of the reductive elimination transition state resulting in a higher activation energy for the coupling of 2-dimethylpropyl with morpholide. Whilst the energy for β-hydride elimination is lower than for morpholide-promoted C–H activation leading to the metallacyclobutane **27**, the increased number of hydrogens available for the latter process could

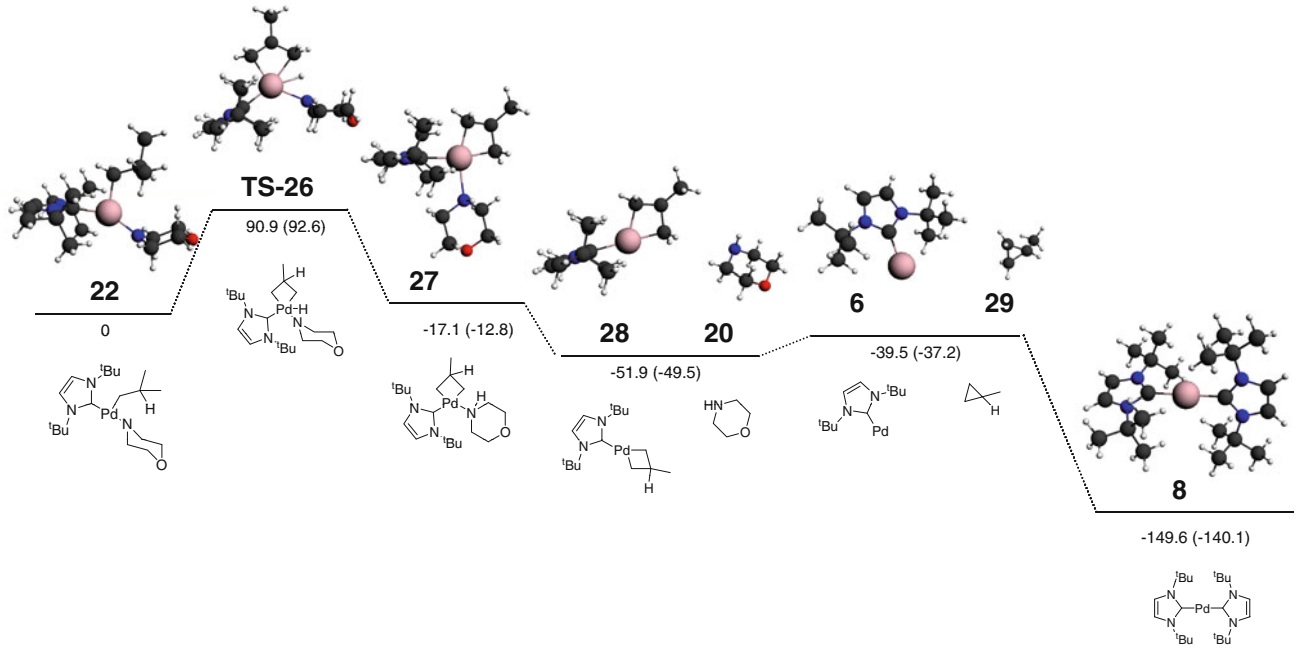

Fig. 5 Calculated relative energy level diagram (kJ mol^{-1}) of the stationary points on the potential energy surface for morpholide-promoted C–H activation of 2-methylpropane in **22**. The energies quoted are gas phase, including zero point, thermal and entropic corrections (at 298.15 K). Values in parentheses are derived from electronic energies computed with the inclusion of solvent effects, with zero point energies, thermal and entropic corrections taken from the gas phase calculations

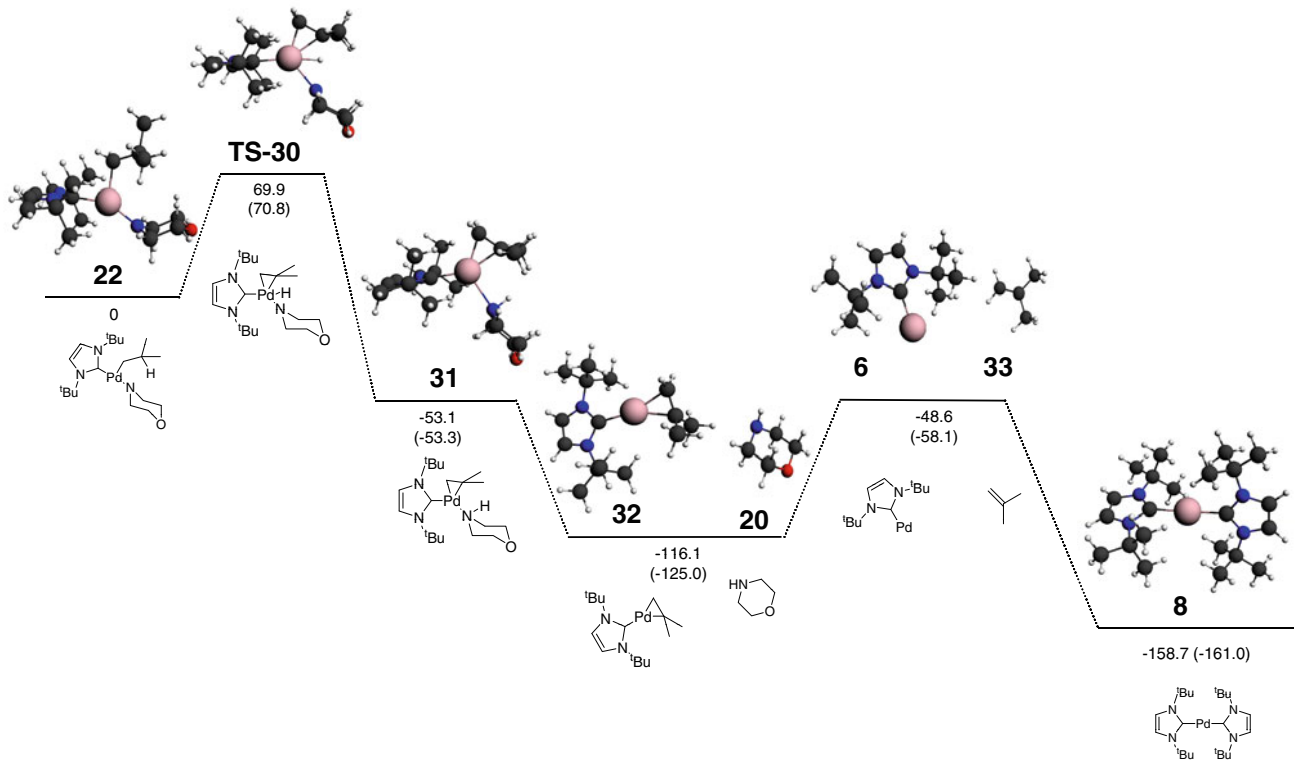

Fig. 6 Calculated relative energy level diagram (kJ mol^{-1}) of the stationary points on the potential energy surface for the β-hydride elimination reaction from 2-methylpropyl in **22**. The energies quoted are gas phase, including zero point, thermal and entropic corrections (at 298.15 K). Values in parentheses are derived from electronic energies computed with the inclusion of solvent effects, with zero point energies, thermal and entropic corrections taken from the gas phase calculations

very well offset this energy difference and make both processes of comparable rate.

4 Conclusions

Our calculations indicate that choosing an alkyl group without β-hydrides, such as neopentyl, in order to inhibit β-hydride elimination, has a detrimental effect on the possibility of (sp^3)C–N reductive elimination; morpholide-promoted C–H activation of neopentyl ^{t}Bu has a significantly lower activation energy than reductive elimination (c. +90 kJ mol^{-1} vs. c. +130 kJ mol^{-1}). Changing the ancillary ligand from I^{t}Bu to P(Cyp)$_3$ in the neopentyl complex has little impact, suggesting that the nature of the alkyl group is the determining factor in the reaction pathway taken, a conclusion supported by the observation that the activation energy for reductive elimination in the analogous phenyl system is less than half that in the neopentyl.

Replacing neopentyl with 2-methylpropyl, to give Pd(I^{t}Bu)(2-methylpropyl)(morpholide), allows us to compare the potential energy surfaces for three possible processes; (1) reductive elimination (2) morpholide-promoted C–H activation and (3) β-hydride elimination. Our calculations indicate that the activation energies for these processes increase in the order (3) < (2) < (1).

We conclude that Pd-catalysed alkyl amination reactions are far from facile. Even in the event of circumventing β-hydride elimination, the reaction is further complicated by morpholide-promoted C–H activation, a previously unreported mechanistic pathway of lower energy than the desired reductive elimination.

Acknowledgments We are grateful to EPSRC and BBSRC for support of this project. We also thank UCL for computing resources via the Research Computing "Legion" cluster and associated services, and the reviewers for their helpful comments.

References

1. Diedrich FS, Stang PJ (1998) Metal-catalysed cross-coupling reactions. Wiley, New York
2. Tsuji J (1995) Reagents and catalysts. Wiley, New York
3. Bellina F, Carpita A, Rossi R (2004) Synthesis-Stuttgart. 2419
4. Miyaura N, Suzuki A (1995) Chem Rev 95:2457
5. Suzuki A (1999) J Organomet Chem 576:147
6. Negishi E, King AO, Okukado N (1977) J Org Chem 42:1821
7. Negishi E, Vanhorn DE (1977) J Am Chem Soc 99:3168
8. O'Brien CJ, Kantchev EAB, Valente C, Hadei N, Chass GA, Lough A, Hopkinson AC, Organ MG (2006) Chem Eur J 12:4743
9. Organ MG, Avola S, Dubovyk I, Hadei N, Kantchev EAB, O'Brien CJ, Valente C (2006) Chem Eur J 12:4749
10. Beletskaya IP, Cheprakov AV (2000) Chem Rev 100:3009
11. Hartwig JF (1998) Acc Chem Res 31:852
12. Tamao K, Sumitani K, Kumada M (1972) J Am Chem Soc 94:4374
13. Wolfe JP, Wagaw S, Marcoux JF, Buchwald SL (1998) Acc Chem Res 31:805
14. Arentsen K, Caddick S, Cloke FGN (2005) Tetrahedron 61:9710
15. Caddick S, Geoffrey F, Cloke N, Hitchcock PB, Leonard J, Lewis AKD, McKerrecher D, Titcomb LR (2002) Organometallics 21:4318
16. Ishiyama T, Abe S, Miyaura N, Suzuki A (1992) Chem Lett 691
17. Zhou J, Fu GC (2004) J Am Chem Soc 126:1340
18. Terao J, Ikumi A, Kuniyasu H, Kambe N (2003) J Am Chem Soc 125:5646
19. Frisch AC, Shaikh N, Zapf A, Beller M (2002) Angew Chem Int Ed 41:4056
20. Jensen AE, Knochel P (2002) J Org Chem 67:79
21. McGuinness DS, Saendig N, Yates BF, Cavell KJ (2001) J Am Chem Soc 123:4029
22. Esposito O, Gois PMP, Lewis A, Caddick S, Cloke FGN, Hitchcock PB (2008) Organometallics 27:6411
23. Esposito O, Lewis A, Hitchcock PB, Caddick S, Cloke FGN (2007) Chem Commun 1157
24. Chass GA, O'Brien CJ, Hadei N, Kantchev EAB, Mu WH, Fang DC, Hopkinson AC, Csizmadia IG, Organ MG (2009) Chem Eur J 15:4281
25. Green JC, Herbert BJ, Lonsdale R (2005) J Organomet Chem 690:6054
26. Surawatanawong P, Fan Y, Hall MB (2008) J Organomet Chem 693:1552
27. Cundari TR, Deng J (2005) J Phys Org Chem 18:417
28. Barder TE, Buchwald SL (2007) J Am Chem Soc 129:12003
29. Goossen LJ, Koley D, Hermann HL, Thiel W (2005) J Am Chem Soc 127:11102
30. Kozuch S, Shaik S (2006) J Am Chem Soc 128:3355
31. Braga AAC, Ujaque G, Maseras F (2006) Organometallics 25:3647
32. Kozuch S, Lee SE, Shaik S (2009) Organometallics 28:1303
33. Goossen LJ, Koley D, Hermann H, Thiel W (2004) Chem Commun 2141
34. Diefenbach A, Bickelhaupt FM (2001) J Chem Phys 115:4030
35. Fazaeli R, Ariafard A, Jamshidi S, Tabatabaie ES, Pishro KA (2007) J Organomet Chem 692:3984
36. Perez-Temprano MH, Nova A, Casares JA, Espinet P (2008) J Am Chem Soc 130:10518
37. Stambuli JP, Incarvito CD, Buhl M, Hartwig JF (2004) J Am Chem Soc 126:1184
38. Ahlquist M, Fristrup P, Tanner D, Norrby PO (2006) Organometallics 25:2066
39. Ahlquist M, Norrby PO (2007) Organometallics 26:550
40. Ariafard A, Lin ZY (2006) Organometallics 25:4030
41. Barder TE, Biscoe MR, Buchwald SL (2007) Organometallics 26:2183
42. Goossen LJ, Koley D, Hermann HL, Thiel W (2005) Organometallics 24:2398
43. Goossen LJ, Koley D, Hermann HL, Thiel W (2006) Organometallics 25:54
44. Senn HM, Ziegler T (2004) Organometallics 23:2980
45. Alvarez R, Faza ON, de Lera AR, Cardenas DJ (2007) Adv Synth Catal 349:887
46. Braga AAC, Morgon NH, Ujaque G, Lledos A, Maseras F (2006) J Organomet Chem 691:4459
47. Braga AAC, Morgon NH, Ujaque G, Maseras F (2005) J Am Chem Soc 127:9298
48. Casares JA, Espinet P, Fuentes B, Salas G (2007) J Am Chem Soc 129:3508
49. Nova A, Ujaque G, Maseras F, Lledos A, Espinet P (2006) J Am Chem Soc 128:14571

50. Napolitano E, Farina V, Persico M (2003) Organometallics 22:4030
51. Ananikov VP, Musaev DG, Morokuma K (2002) J Am Chem Soc 124:2839
52. Ananikov VP, Musaev DG, Morokuma K (2005) Organometallics 24:715
53. Zuidema E, van Leeuwen P, Bo C (2005) Organometallics 24:3703
54. Macgregor SA, Neave GW, Smith C (2003) Faraday Discuss 124:111
55. Scientific Computing and Modelling, Theoretical Chemistry, Vrei Universiteit, Amsterdam, The Netherlands, http://www.scm.com
56. Perdew JP, Burke K, Ernzerhof M (1996) Phys Rev Lett 77:3865
57. Perdew JP, Burke K, Ernzerhof M (1997) Phys Rev Lett 78:1396
58. Evans WJ, Kozimor SA, Ziller JW, Kaltsoyannis N (2004) J Am Chem Soc 126:14533
59. Häller J, Kaltsoyannis N, Sarsfield MJ, May I, Cornet S, Redmond M, Helliwell M (2007) Inorg Chem 46:4868
60. Gaunt AJ, Reilly SD, Enriquez AE, Scott BL, Ibers JA, Sekar P, Ingram KIM, Kaltsoyannis N, Neu MP (2008) Inorg Chem 47:29
61. Ingram KIM, Tassell MJ, Gaunt AJ, Kaltsoyannis N (2008) Inorg Chem 47:7824
62. Tassell MJ, Kaltsoyannis N (2010) Dalton Trans. doi:10.1039/c000704h
63. Klamt A (1995) J Phys Chem 99:2224
64. Klamt A, Schuurmann G (1993) J Chem Soc Perkin Trans 2 **5**, 799
65. Lewis AKD, Caddick S, Cloke FGN, Billingham NC, Hitchcock PB, Leonard J (2003) J Am Chem Soc 125:10066
66. Mayer I (1984) Int J Quant Chem 26:151
67. Mayer I (1983) Chem Phys Lett 97:270
68. Cavigliasso G, Bridgeman AJ, Ireland LR, Rothery J (2001) J Chem Soc Dalton Trans 2095
69. Brainard RL, Miller TM, Whitesides GM (1986) Organometallics 5:1481
70. Diversi P, Fasce D, Santini R (1984) J Organomet Chem 269:285
71. Miyashita A, Ohyoshi M, Shitara H, Nohira H (1988) J Organomet Chem 338:103